Purification of Single-Photon Entanglement

D. Salart,[1] O. Landry,[1] N. Sangouard,[1] N. Gisin,[1] H. Herrmann,[2] B. Sanguinetti,[1] C. Simon,[1,*] W. Sohler,[2] R. T. Thew,[1] A. Thomas,[2] and H. Zbinden[1]

[1]*Group of Applied Physics, University of Geneva, 20, Rue de l'Ecole de Médecine, CH-1211 Geneva 4, Switzerland*
[2]*Universität Paderborn, Fakultät für Naturwissenschaften, Department Physik, Warburger Straße 100 33098 Paderborn, Germany*
(Received 25 January 2010; revised manuscript received 26 March 2010; published 6 May 2010)

Single-photon entanglement is a simple form of entanglement that exists between two spatial modes sharing a single photon. Despite its elementary form, it provides a resource as useful as polarization-entangled photons and it can be used for quantum teleportation and entanglement swapping operations. Here, we report the first experiment where single-photon entanglement is purified with a simple linear-optics based protocol. In addition to its conceptual interest, this result might find applications in long distance quantum communication based on quantum repeaters.

DOI: 10.1103/PhysRevLett.104.180504 PACS numbers: 03.67.Bg, 42.50.Dv, 42.50.Ex

Entanglement purification provides a fascinating conceptual viewpoint to gain insight into the properties of entanglement. It can be used for the quantification of entanglement in bipartite systems [1]. It may also be useful in practical applications, e.g., in the context of long distance quantum communication where the direct transmission of photons through an optical fiber is limited by losses and the no-cloning theorem. This can be overcome using quantum repeaters [2], which require the creation of entanglement over short links, the storage of entangled states within these links, and entanglement swapping operations to distribute entangled states over longer distances. In practice, these operations introduce errors, limiting the number of links that can be used. While the most immediate goal of outperforming the direct transmission may not need purification, the entanglement distribution within future quantum networks requires a larger number of links, necessitating several purification operations [3].

Initial proposals by Bennett *et al.* [4] and Deutsch *et al.* [5] for entanglement purification were expressed in terms of quantum gates. For practical applications, e.g., in the frame of quantum repeaters, it is important to keep implementations as simple as possible. For example, the protocol presented in Ref. [6] and implemented as reported in Ref. [7] requires linear optical elements only, and can easily be integrated into quantum repeater architectures. However, this last proposal is suited to the purification of polarization-entangled pairs of photons whereas many attractive quantum repeater protocols [8–10] and related experiments [11,12] use single-photon entanglement, i.e., entanglement of the form $|1\rangle_A|0\rangle_B + |0\rangle_A|1\rangle_B$, where two modes A and B share a single photon. First, these repeaters are rather simple: they require significantly fewer resources than other protocols and are thus less sensitive to memory and photon detector inefficiencies [3]. Furthermore, these quantum repeaters are efficient since they offer high entanglement distribution rates when combined with temporal multiplexing [9]. The main drawback of protocols based on single-photon detections is that, unlike protocols based on two-photon detections, they are interferometrically sensitive to path length fluctuations [13] that are at the origin of phase errors. An active stabilization system, such as the one reported in [14], would be required. However, remaining path length fluctuations and additional phase noise coming from unfaithful quantum memories and imperfections in entanglement swapping operations would likely require purification. Here, we report the first experimental implementation of a protocol for phase-error purification of single-photon entanglement based on linear optics.

The principle of purification for phase errors (see Ref. [15] for details) can be illustrated as follows. Alice and Bob, two protagonists located at remote locations A and B respectively, wish to share a maximally entangled state $\psi_+^{ab} = \frac{1}{\sqrt{2}}(|1\rangle_A|0\rangle_B + |0\rangle_A|1\rangle_B) \equiv \frac{1}{\sqrt{2}}(a^\dagger + b^\dagger)|0\rangle$, but due to phase errors, they share a state which has an admixture of the singlet state ψ_-^{ab}

$$\rho_{ab} = F|\psi_+^{ab}\rangle\langle\psi_+^{ab}| + (1-F)|\psi_-^{ab}\rangle\langle\psi_-^{ab}|. \qquad (1)$$

F is the fidelity of the shared state: if $F = 1/2$, the phase information is lost and no entanglement is left while in the case where $F = 1$, the state is maximally entangled. Note that these phase errors are the most important. The empty component $|0\rangle_A|0\rangle_B$ does not affect the fidelity of the distributed state since the final step of single-photon protocols postselects the cases where there was a photon in the output state [8]. The multiphoton components $|1\rangle_A|1\rangle_B$ can be greatly reduced using specific architectures [10].

Suppose that Alice and Bob share two copies of the state described by (1), $\rho_{a_1b_1}$ with fidelity F_1 and $\rho_{a_2b_2}$ with fidelity F_2 (see Fig. 1). Alice and Bob both perform unitary transformations on their modes a_1, a_2 and b_1, b_2 respectively: Alice combines the two modes a_1, a_2 on a beam splitter with an intensity transmission of 85% and Bob uses a beam splitter with an intensity transmission of 15%. The detection of a single photon by Alice in mode d_a (or by Bob in mode d_b), projects the modes $\tilde{a}$, $\tilde{b}$ on a mixed state

 © 2010 The American Physical Society

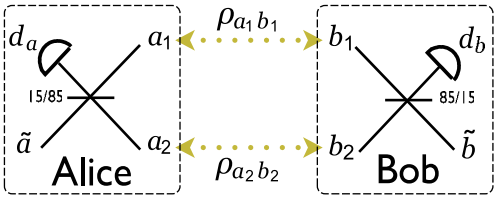

FIG. 1 (color online). Scheme for entanglement purification of single-photon entanglement. Alice and Bob share two entangled single-photon states $\rho_{a_1 b_1}$, $\rho_{a_2 b_2}$ [of the form given in Eq. (1)] with fidelity F_1 and F_2, respectively. While Alice combines the modes a_1 and a_2 on a 15/85 beam splitter, Bob couples the modes b_1 and b_2 on a 85/15 beam splitter. The detection of one photon in either d_a or d_b projects the modes $\tilde{a}$ and $\tilde{b}$ into a single-photon entangled state $\rho_{\tilde{a}\tilde{b}}$ with higher fidelity $\tilde{F}$.

$\rho_{\tilde{a}\tilde{b}}$ with fidelity [15]

$$\tilde{F} = \frac{F_1 F_2 + F_1/2 + F_2/2}{1 + F_1 F_2 + (1 - F_1)(1 - F_2)}. \tag{2}$$

Remarkably, the state resulting from this simple operation is substantially purified. As an example, if errors are of the order of ϵ, i.e., $F_1 = F_2 = 1 - \epsilon$, the purification protocol divides them by a factor of 2, i.e., $\tilde{F} = 1 - \epsilon/2 + o(\epsilon^2)$. In quantum repeaters the error is approximately doubled with every level of entanglement swapping. The present protocol has the potential to significantly increase the number of possible levels, and thus the achievable distance. Furthermore, in principle, the protocol could be applied again to the already purified states, and this process could continue as long as there are entangled states remaining, obtaining an increasingly purified state at every step. Note that the success probability for the purification protocol is $p = \frac{1}{4}[1 + F_1 F_2 + (1 - F_1)(1 - F_2)]$ which is close to 1/2 for values of F_1 and F_2 that are close to 1. Note also that the previously mentioned proposal [6] based on polarization entanglement squares the errors, i.e., $\tilde{F} = 1 - \epsilon^2 + o(\epsilon^3)$. We have shown that our scheme achieves the optimal fidelity (see Ref. [15] for a detailed discussion) for single-photon entanglement. This protocol reveals an intrinsic difference between single-photon entanglement and polarization-entangled photons.

The physics behind the purification is based on the interference of two modes sharing a single photon and on the bosonic character of indistinguishable photons. Single-photon interference requires a stable setup. Phase oscillations need to be kept under certain control in order to apply the purification protocol successfully. Indeed, there needs to be some initial entanglement left to purify. For a kilometer long interferometer, active stabilization would likely be required. In our experiment, where interferometer arms are 10 m long, phase oscillations are minimized by controlling the temperature. Indistinguishability of the photons demands a good overlap of the temporal, spectral, spatial and polarization modes of the photons. Thus, the successful construction and operation of an experimental setup that provided both indistinguishable photons and high visibility single-photon interference allows us, for the first time, to demonstrate the purification of single-photon entanglement.

The experimental setup is shown in Fig. 2. A Ti-indiffused 7 μm wide waveguide in 25 mm long periodically poled ($\Lambda = 9.15$ μm) lithium niobate (Ti:PPLN) operated at 43 °C—monomode around 1.5 μm wavelength—creates degenerate photon pairs through the process of spontaneous parametric down conversion. The periodicity of Λ has been chosen to obtain "type-II" quasi-phase-matching for orthogonally polarized signal and idler photons. The waveguide is pumped by a continuous-wave single-mode external cavity diode laser at 780 nm (Toptica DL100). After the waveguide, the remaining light from the pump laser is blocked by a silicon filter. The signal and idler photons, with a spectral width of 3 nm (full width at half maximum) centered at 1560 nm, both pass through the same narrowband filter with a bandwidth of 1.3 nm reducing their spectral distinguishability. The photons are then separated with a polarizing beam splitter (PBS) and coupled into single-mode optical fibers. Each photon is sent through a 50/50 coupler (BS1 and BS2) to prepare the two-mode entangled states $\rho_{a_1 b_1}$ and $\rho_{a_2 b_2}$. These states are then distributed between Alice and Bob. They each receive two modes, one from each entangled state, and combine them using couplers BS4 and BS5, respectively. These last two couplers are manual

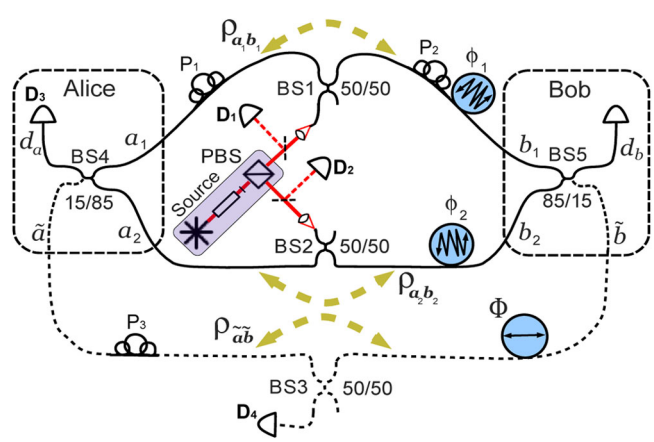

FIG. 2 (color online). Experimental setup. Pairs of orthogonally polarized photons are created by a waveguide-based source, separated by a PBS and coupled into optical fibers. Each photon passes through a 50/50 coupler (BS1 and BS2) to create two-mode entangled states $\rho_{a_1 b_1}$ and $\rho_{a_2 b_2}$. Alice and Bob each receive two modes, one from each state, and combine them using 15/85 couplers (BS4 and BS5). Conditional on the detection of one photon by either Alice or Bob, a purified single-photon entangled state $\rho_{\tilde{a}\tilde{b}}$ is created. The degree of entanglement is measured using the 50/50 coupler BS3. Two noise generators (ϕ_1 and ϕ_2) are used to reduce the fidelities F_1 and F_2 of $\rho_{a_1 b_1}$ and $\rho_{a_2 b_2}$, respectively. The phase Φ is scanned using a piezo to acquire an interferogram and thus estimate the fidelities.

variable-ratio evanescent wave couplers (Canadian Instrumentation & Research Ltd).

Finally, for all measurements we use two single-photon detectors: the heralding detector is a free-running InGaAs/InP avalanche photodiode with homemade electronics [16]. Depending on the measurement, this detector is at positions D_1, D_2 or D_3 in Fig. 2. The quantum efficiency is 10.2% with 1.3 kHz of dark counts for a temperature of $-50\,^{\circ}$C and a bias voltage of -48.5 V. Its *effective* efficiency decreases as the number of singles increases, since the detection rate is limited by a dead time of 31 μs. The triggered detector is an InGaAs avalanche photodiode (idQuantique, id200) working in gated mode and operated at an efficiency of 5.5%, 2.7×10^{-5} dark counts $\cdot$ ns^{-1} and a dead time of 10 μs.

The efficiency of the photon pair source is determined by calculating the number of photon pairs that are created. We measure 15.5 kHz of singles at detector D_1, an effective detector efficiency of 5.3% and a transmission of 0.077 between the waveguide and detector D_1. We generate approximately 4×10^6 pairs $\cdot$ s^{-1} for a spectral width of 1.3 nm from a pump power of 16 mW at 780 nm. This is equivalent to $p = 3.2 \times 10^{-3}$ pairs per detection time window of $\tau_d = 800$ ps. The detection time window is the FWHM of the coincidence peak and it depends primarily on the jitter of the single-photon detectors.

The degree of indistinguishability of the two photons can be measured through the visibility of the Hong-Ou-Mandel (HOM) dip [17]. If the photons were perfectly indistinguishable, the number of coincidences would be zero and the visibility of the HOM dip would be 100%. We have estimated, using a simple model with discrete modes, that the presented protocol requires overlaps between the distributions associated to the modes a_1, a_2, b_1 and b_2 above 90% to obtain a significant purification effect. The temporal overlap between the modes is achieved by adjusting the path lengths that each photon has to travel between the PBS and the couplers BS3, BS4, and BS5. The spectral overlap is ensured due to both photons passing through the same narrowband filter. The use of single-mode fibers guarantees the transverse spatial overlap. Lastly, the polarization is controlled using the polarization controllers shown in Fig. 2. After performing these adjustments, we observed a HOM dip with the extremely high visibility of $V_{\mathrm{dip}} = (C_{\max} - C_{\min})/C_{\max} = (99.0 \pm 0.3)\%$.

To determine the degree of entanglement for $\rho_{a_1 b_1}$, we measure the visibility V_1 of interference fringes. The visibility is a good measure of the fidelity $F_1 = (1 + V_1)/2$ of the state $\rho_{a_1 b_1}$ since we postselect the cases where there is at least one excitation in either a_1 or b_1 and since the probability of multipair emissions is low, as confirmed by the visibility of the HOM dip. To herald the creation of the state $\rho_{a_1 b_1}$ at coupler BS1, the photon reflected at the PBS is not sent to BS2 but detected by D_2. Its modes a_1, b_1 are sent to Alice and Bob, respectively, and then combined using the auxiliary measurement interferometer (depicted as dotted lines in Fig. 2) that leads to coupler BS3 and detected at D_4. The path chosen by the single photon is unknown, leading to interference fringes when the phase Φ of the interferometer is scanned. To scan this phase, we use a circular piezoelectric actuator with optical fiber coiled around it. A voltage ramp is applied to the piezo that progressively expands, stretching the fiber and changing the phase. To determine the degree of entanglement for $\rho_{a_2 b_2}$, the measurement is repeated, inverting the roles for the transmitted and reflected photons at the PBS. We measured the initial fidelity of $\rho_{a_1 b_1}$ as $F_1 = (97.8 \pm 0.2)\%$ while $\rho_{a_2 b_2}$ has a fidelity $F_2 = (97.7 \pm 0.2)\%$. The residual 2% is mainly due to path length instabilities (see the supplementary information in Ref. [18]).

This purification protocol works for a wide range of fidelities F_1 and F_2, but it is at fidelities close to $F_1 = F_2 = 76\%$ where the fidelity increase is greatest [15]. To reduce the initial fidelities, we generate noise in a controlled and reproducible way with two additional circular piezos (ϕ_1 for state $\rho_{a_1 b_1}$ and ϕ_2 for state $\rho_{a_2 b_2}$) that vibrate at a frequency much higher than the integration time of the measurement. This noise is independently generated for each piezo. We chose a function that reproduces the Gaussian phase-noise distribution in a fiber, as observed in real world networks [13]. Interference fringes measured in one of the entangled states and the reduction of the fidelity due to the noise generation are shown in Fig. 3(a). After applying the noise, the fidelities reduce to $F_1 = (75.1 \pm 0.8)\%$ and $F_2 = (75.0 \pm 0.7)\%$.

To prepare the purified state, the variable couplers BS4 and BS5 are adjusted to the intensity transmissions re-

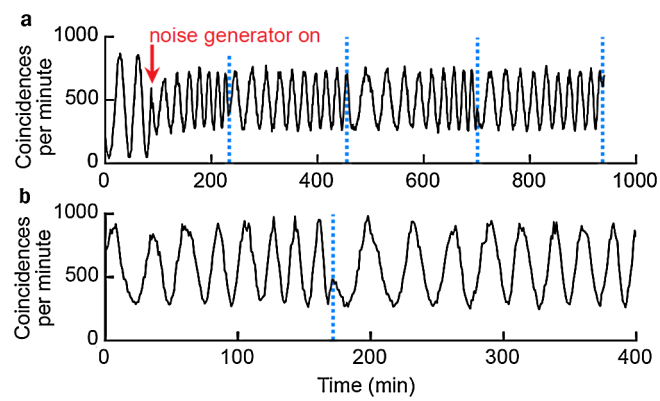

FIG. 3 (color online). Raw interference fringes observed while the phase Φ is being scanned. (a) Coincidences between detectors D_1 (herald) and D_4 corresponding to the state $\rho_{a_2 b_2}$. Initially, the fidelity is $F_2 = (97.7 \pm 0.2)\%$. When the noise generator ϕ_2 is switched on, the fidelity decreases to $F_2 = (75.0 \pm 0.7)\%$. (b) Coincidences between detectors D_3 and D_4 corresponding to the purified state $\rho_{\tilde{a}\tilde{b}}$. While both noise generators are on, the fidelity is $\tilde{F} = (79.6 \pm 1.1)\%$. These values are obtained after the subtraction of accidental coincidences due to dark counts. Even when they are not subtracted, a definite purification effect can still be observed. The vertical lines mark every time the voltage ramp reaches its end, reversing the scan direction.

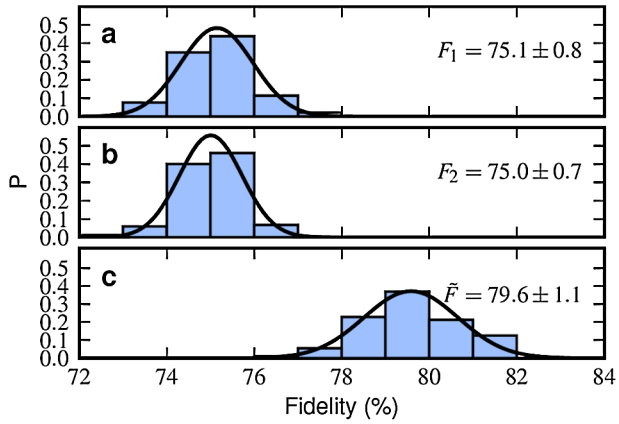

FIG. 4 (color online). Distribution of the fidelity measurements. Probability densities P as a function of the measured fidelities for (a) state $\rho_{a_1 b_1}$, (b) state $\rho_{a_2 b_2}$ and (c) the purified state $\rho_{\tilde{a}\tilde{b}}$. The corresponding mean fidelity and standard deviation are given next to each distribution. The curves are Gaussian functions with the same mean and σ as the sample data. The number of bins chosen is the optimal one using Scott's principle [22]. The agreement with the histogram can be seen by the fact that the fitted curve passes through the center of most histogram bars.

quired to apply the purification protocol [15], corresponding to 85% for Alice and 15% for Bob (or vice versa). Modes a_1 and a_2 are combined by Alice to form modes $\tilde{a}$ and d_a, while modes b_1 and b_2 are combined by Bob to form modes $\tilde{b}$ and d_b. Conditioned on the detection of one photon at d_a (with detector D_3), modes $\tilde{a}$ and $\tilde{b}$ become purified. To verify this, they are combined at coupler BS3 and detected at D_4. Again, because we cannot know which path the photons have taken, interference fringes are observed when the phase Φ is scanned [see Fig. 3(b)]. As before, the fidelity $\tilde{F}$ of the state $\rho_{\tilde{a}\tilde{b}}$ is deduced from the visibility of the fringes.

For each of the entangled states ($\rho_{a_1 b_1}$, $\rho_{a_2 b_2}$ and $\rho_{\tilde{a}\tilde{b}}$), measurements of several interference fringes were obtained. Using sequential sinusoidal fits of approximately two periods, we calculated the fidelities for all fringes. The resulting distributions of fidelity values are represented in Fig. 4. From each set of values, the mean fidelities F_1, F_2, and $\tilde{F}$ were calculated. The given uncertainty values are the standard deviations (σ) associated with each distribution [18].

After the implementation of the purification protocol, we obtain a state $\rho_{\tilde{a}\tilde{b}}$ with fidelity $\tilde{F} = (79.6 \pm 1.1)\%$. The improvement in the degree of entanglement, taken as the difference between $\tilde{F}$ and F_1, is as high as 4.5%. Note that it has been shown in Ref. [15] that the optimal theoretical value is of 5.7%. We believe that the remaining 1.2% is due to phase fluctuations of modes and to the uncertainty in the transmission of variable couplers [18]. As shown in Fig. 4, the overlap between the distributions of initial and purified fidelity values is negligible, leaving no doubt about the influence of the purification effect.

Single-photon entanglement has been at the heart of a lively debate [19,20]. Part of the controversy has been solved by mapping single-photon entanglement into two atomic ensembles and by revealing the entanglement between these ensembles [12]. Note also that entanglement between four modes sharing a single photon has been characterized by direct measurements of the optical modes [21]. Our experiment further shows that single-photon entanglement can be purified using linear optics. Looking further ahead, this simple protocol could be useful in the context of quantum repeaters.

We thank C. Barreiro and J.-D. Gautier for technical support and H. de Riedmatten for his insightful comments and careful reading of the manuscript. This work was supported by the Swiss NCCR Quantum Photonics and the European Union projects QAP and ERC-AG QORE.

*Present address: Institute for Quantum Information Science and Department of Physics and Astronomy, University of Calgary, 2500 University Drive NW, Calgary T2N 1N4, Alberta, Canada.

[1] R. Horodecki *et al.*, Rev. Mod. Phys. **81**, 865 (2009).
[2] H.-J. Briegel *et al.*, Phys. Rev. Lett. **81**, 5932 (1998).
[3] N. Sangouard *et al.*, arXiv:0906.2699.
[4] C. H. Bennett *et al.*, Phys. Rev. Lett. **76**, 722 (1996).
[5] D. Deutsch *et al.*, Phys. Rev. Lett. **77**, 2818 (1996).
[6] J.-W. Pan *et al.*, Nature (London) **410**, 1067 (2001).
[7] J.-W. Pan *et al.*, Nature (London) **423**, 417 (2003).
[8] L.-M. Duan *et al.*, Nature (London) **414**, 413 (2001).
[9] C. Simon *et al.*, Phys. Rev. Lett. **98**, 190503 (2007).
[10] N. Sangouard *et al.*, Phys. Rev. A **76**, 050301(R) (2007).
[11] C.-W. Chou *et al.*, Nature (London) **438**, 828 (2005); C.-W. Chou *et al.*, Science **316**, 1316 (2007).
[12] K. S. Choi *et al.*, Nature (London) **452**, 67 (2008).
[13] J. Minář *et al.*, Phys. Rev. A **77**, 052325 (2008).
[14] S.-B. Cho, and T.-G. Noh, Opt. Express **17**, 19027 (2009).
[15] N. Sangouard *et al.*, Phys. Rev. A **78**, 050301(R) (2008).
[16] R. T. Thew *et al.*, Appl. Phys. Lett. **91**, 201114 (2007).
[17] C. K. Hong, Z. Y. Ou, and L. Mandel, Phys. Rev. Lett. **59**, 2044 (1987).
[18] See supplementary material at http://link.aps.org/supplemental/10.1103/PhysRevLett.104.180504 for more detailed information about the measurement procedure, the data analysis, accidental coincidences and the imperfect HOM dip visibility and fidelities.
[19] S. M. Tan, D. F. Walls, and M. J. Collett, Phys. Rev. Lett. **66**, 252 (1991).
[20] S. J. van Enk, Phys. Rev. A **72**, 064306 (2005) and references therein.
[21] S. B. Papp *et al.*, Science **324**, 764 (2009).
[22] D. W. Scott, Biometrika **66**, 605 (1979).